Springer

KSME

Journal of Mechanical Science and Technology 28(8) (2014) 3825~3835
www.springerlink.com/content/1738-494x
DOI 10.1007/s12206-014-0846-3

Nonlinear transient heat conduction analysis of hollow thick temperature-dependent 2D-FGM cylinders with finite length using numerical method †

Mohammad Hassan Shojaeefard[1] and Amir Najibi[2,*]

[1]*School of Mechanical Engineering, Iran University of Science & Technology, Tehran, Iran*
[2]*School of Automotive Engineering, Iran University of Science & Technology, Tehran, Iran*

(Manuscript Received February 24, 2013; Revised April 10, 2014; Accepted May 19, 2014)

Abstract

Nonlinear transient heat conduction analysis is developed for hollow thick temperature-dependent 2D-FGM cylinders subjected to transient non-uniform axisymmetric thermal loads. It is demonstrated here that the temperature-dependency in addition to the material properties variation in the 2D- FGM would lead to highly nonlinear governing equations. To do this, the graded finite element method is employed to model the structures and a quadratic Lagrange shape function has been used to improve the accuracy of the temperature distribution for the two-dimensional heat conduction analysis. Furthermore, time variation of the temperatures and the effects of material distribution variability in two radial and axial directions and the temperature-dependency of the material properties on the temperature are discussed in detail. It is assumed that the material, geometry and volume fraction distribution are axisymmetric but not uniform along the axial direction. According to the results, the variation of the material properties in two dimensions has significant effect on temperature distribution; therefore, it gives more designing flexibility benefits to the designers to implement this kind of material for the thermal barriers purposes.

Keywords: 2D-FGM; Thick hollow cylinder; Temperature dependent properties; Transient heat conduction

1. Introduction

To deal with high temperature ranges which exist inevitably in many industrial machine components, including space shuttles, combustion engines, nuclear power plants and ovens, necessitates having more high temperature resistant materials for improving the strength of such machine elements. In recent years, the concept of a functionally graded material (FGM) has been introduced as thermal barrier materials, which the continuity of their material properties prevents cracking, stress singularities and separations of the interface that are drawbacks of the multi-layer composite plates commonly used as thermal barriers in machines and equipment [1, 2]. In fact, the low thermal conductivity, low coefficients of thermal expansion, core ductility, and smooth stress distribution have enabled the FGMs to withstand higher thermal and mechanical shocks [3, 4]. However, transient thermal analysis is a fundamental stage in development of thermomechanical investigations such as dynamic thermal buckling, fatigue life assessment under cyclic thermal loads, dynamic crack propagation, etc.; most of the well-known thermoelastic analyses have been conducted so far for the thick FGM cylinders which are generally restricted to a uniform heating (e.g. [5]) or steady-state heat transfer conditions [6-11]. Some of these researches have been accomplished based on the multi-layer discretization approximation [10].

Although, in those aforementioned studies, transient heat transfer analysis for the FGM cylinders is very limited and thus most of them have ignored the temperature-dependency of the material properties, but Reddy and Chin [12] have developed Lagrangian finite element formulations time integration method to analyze the pseudo-dynamic thermoelastic responses of the functionally graded cylinders.

The transient thermal stress problem by using a laminated composite model was studied by Ootao et.al. The effects of non-homogeneity of material on the stress distribution were also investigated [13]. Haw-Long Lee et al., investigated temperature distributions and thermal stresses in a functionally graded hollow cylinder under simultaneous inner and outer boundary heat flux [14]. Hosseini et al., investigated thermoelastic waves propagation in functionally graded hollow cylinder based on Green-Naghdi model of coupled thermoelasticity [15]. Tariq Darabsehet. al., studied transient thermoelasticity response of an FG hollow cylinder subjected to thermal loading based on Green-Lindsay model [16]. Temperature distri-

*Corresponding author. Tel.: +98 21 6657 6447, Fax.: +98 21 88013029
E-mail address: najibi@iust.ac.ir
† Recommended by Associate Editor Dae Hee Lee

bution in a functionally graded hollow cylinder under a transient-state temperature field based on thermal elasticity theory and the arbitrary difference precise integration (ADPI) has been investigated by Xiao-dan Zhang in 2012 [17].

Awaji and Sivakumar [18] used the finite difference method to analyze the steady-state and transient temperature distributions in a FGM cylinder. Kim and Noda, based on the multi-layered cylinder approximation, studied an axisymmetric two-dimensional transient thermoelasticity for an infinite hollow circular FGM cylinder using Green's function approach [19]. Sladek et al. [20] studied the transient heat conduction in the FGM cylinders by the numerical Laplace inversion method. Wang et al. [21, 22] used the first-order finite element in conjunction with the finite difference method to study the one-dimensional transient heat conduction. Hosseini et al. [23], and Shao and Ma [24] employed analytical methods to study the transient conduction heat transfer in FGM cylinders with material properties that follow an exponential law. Thermo-mechanical analysis of an FGM hollow circular cylinder subjected to a linearly increasing boundary temperature was developed by Shao and Ma [25]. Thermo-mechanical properties of the FGMs were assumed to be temperature-independent, and also both Laplace transform technique and a series method were employed to solve the ordinary differential equations of the FGM cylinders with material properties that follow as an exponential law.

Since most functionally graded structures are commonly used in a high temperature environment where a range of significant changes in mechanical properties of the constituent materials can be expected [12], it is essential to take into consideration this temperature-dependency for accurate prediction of the mechanical response. Thus, the effective material properties are assumed to be temperature dependent and can be expressed as a nonlinear function of temperature [26].

Accordingly, Shariyat [27-29] investigated numerically some aspects of the vibration and wave propagation phenomena in thick hollow functionally graded cylinders with temperature-dependent material properties under thermo-mechanical loads.

As it is mentioned above, the variation of the volume fraction and properties of the FGMs are in one-dimensional and the material properties vary continuously from one surface to the other with a prescribed function in all cases, while in the advanced machine elements the thermal and mechanical loading may change in two or three directions. Based on this fact, two-dimensional (2D) FGM, of which material properties are bi-directionally dependent is introduced [30]. Cho and Ha [31] characterized thermoelasticbehavior of heat resisting FGMs, under given thermal loading and boundary conditions by spatial distribution of volume fractions related to the constituent particles. They addressed a 2D volume-fraction optimization procedure for relaxing the effective thermal stress distribution. Furthermore, the reduction of thermal stresses in a plate using new developed 2D-FGMs was investigated by Nemat-Alla [32].

In his study, a 2D-FGM rectangular plate under transient thermal loading is considered and also the finite element method is used to solve the governing equations. Elastic-plastic analysis of 2D FGMs under thermal loading in a plate was also studied by Nemat-Alla et al., in which the material properties were considered to be temperature dependent [33]. Duo to the nonlinear governing equations, the finite element method is a common approach for solving this kind of problems in the literatures. Although, it should be noted, the use of a single material property for each element within an individual element will result in a significant discontinuity and thus inaccuracies for transient and dynamic problems [34]. These inaccuracies will be more significant in 2D-FGM cases. Sentare et al. showed that graded finite element can improve the accuracy without increasing the number of degrees of freedom and decreasing the elements' size [34].

Analysis of transient heat conduction of a thick hollow functionally graded cylinder with finite length is rarely seen in the literature. Also, the heat conduction in finite length cylinder is often investigated only in radial direction in these cases, while in real situations the heat conduction can be 2D in a finite length cylinder. On the other hand, in all cases the material gradation of FGM is 1D. Therefore, analysis of heat transient conduction of a thick hollow cylinder made of 2D FGM can be of great importance [35].

In this paper, a nonlinear transient heat conduction analysis of a thick hollow 2D functionally graded cylinder with finite length and temperature-dependent material properties subjected to transient thermal loading conditions is presented. The variation of the material properties in 2D and the nonlinear temperature dependency of the material beside the graded finite element with second order Lagrange shape functions are the novelty of this study. Accordingly, first, a graded finite element transient heat conduction analysis was performed and then the results were verified with similar example in the literature.

Second, the graded finite element analysis was performed to solve both of the transient heat conduction equation and the verification according to the previous literature was carried out. Furthermore, the material distribution graph and time variation of the temperature in different power law coefficients were demonstrated.

Finally, those results based on the assumptions of temperature-dependency (TD) and temperature-independency (TID) of the material properties were compared with each other as well as the effects of various parameters on the transient responses are investigated.

2. Problem formulation

In this section, the governing equations of heat transfer in axisymmetric cylindrical coordinates are obtained. Volume fraction distributions in the two radial and axial directions are introduced and graded finite element is used for modelling of the material non-homogeneity. Consider a 2D-FGM thick

hollow cylinder of internal radius a, external radius b, and finite length L. Because of the axisymmetry of the geometry and loading, coordinates r and z are used in the analysis.

2.1 Heat transfer equations

Without existence of heat sources, the equation of heat conduction in axisymmetric cylinder coordinates is demonstrated as [35]:

$$\frac{1}{r}\frac{\partial}{\partial r}\left(rk(r,z,T)\frac{\partial T(r,z,t)}{\partial r}\right)+\frac{\partial}{\partial z}\left(k(r,z,T)\frac{\partial T(r,z,t)}{\partial z}\right)=\rho(r,z,T)c(r,z,T)\frac{\partial T(r,z,t)}{\partial t}, \tag{1}$$

where $k(r, z, T)$, $\rho(r, z, T)$ and $c(r, z, T)$ are thermal conductivity, mass density and heat capacity of functionally graded material, respectively. The thermal conductivity tensor is diagonal and $k_{rr}(r, z, T) = k_{zz}(r, z, T) = k(r, z, T)$. The thermal boundary conditions are:

$$T(r=a,z,t)=T_0(1-e^{c_0 t})\sin\left(\frac{\pi z}{L}\right), \tag{2}$$

$$k\frac{\partial T(r=b,z,t)}{\partial r}+h_0(T-T_\infty)=0, \tag{3}$$

$$-k\frac{\partial T(r,z=0,t)}{\partial z}+h_L(T-T_\infty)=0, \tag{4}$$

$$k\frac{\partial T(r,z=L,t)}{\partial z}+h_U(T-T_\infty)=0, \tag{5}$$

where Eq. (2) shows the temperature at the inner radius and Eqs. (3)-(5) show heat convection at the outer, lower and top surface, respectively. h_0, h_L and h_U are convection coefficients in outerside, lower and upper surfaces, respectively. T_∞ is the surrounding temperature, and T_0 and c_0 are constant values. It is assumed that the cylinder is exposed to the uniform initial temperature.

2.2 Volume fraction and material distribution in 2D-FGM cylinder

Two-dimensional FGMs are usually made by continuous gradation of three or four distinct material phases in which one or two of them are ceramics and the others are metal alloy phases. The volume fractions of the constituents vary in a predetermined composition profile.

Now if we consider the volume fractions of 2D-FGM at any arbitrary point in the 2D-FGM axisymmetric cylinder shown in Fig. 1, the volume fraction of the first ceramic material is changed from 100% at the lower surface to zero at the upper surface by a power law function which, in the present cylinder, the inner surface is made of two distinct ceramics and the outer surface from two metals. Also, this volume fraction changes continuously from inner surface to the outer surface. Moreover, volume fractions of the other materials are changed similar to the one mentioned, in two directions. The volume fraction distributions of each material can be expressed as [35]:

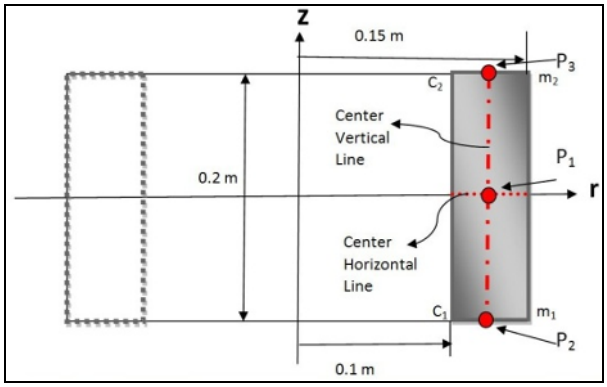

Fig. 1. 2D-FGM and material distribution of the axisymmetric cylinder with predetermined points and lines.

$$V_{c1}=\left[1-\left(\frac{r-a}{b-a}\right)^{n_r}\right]\left[1-\left(\frac{z}{L}\right)^{n_z}\right], \tag{6a}$$

$$V_{c2}=\left[1-\left(\frac{r-a}{b-a}\right)^{n_r}\right]\left[\left(\frac{z}{L}\right)^{n_z}\right], \tag{6b}$$

$$V_{m1}=\left[\left(\frac{r-a}{b-a}\right)^{n_r}\right]\left[1-\left(\frac{z}{L}\right)^{n_z}\right], \tag{6c}$$

$$V_{m2}=\left[\left(\frac{r-a}{b-a}\right)^{n_r}\right]\left[\left(\frac{z}{L}\right)^{n_z}\right], \tag{6d}$$

where subscripts c1, c2, m1 and m2 denote the first and second ceramic and the first and second metal, respectively. Also, n_r and n_z are those parameters that represent the basic constituent distributions in r and z-directions.

To accurately model the material properties of FGMs, the properties must be temperature- and position-dependent. This is achieved by using a simple rule of mixture of composite materials (Voigt model [36]). The effective material properties P of the FGM, like conductivity coefficient k, and thermal expansion coefficient α, can then be expressed as [36]:

$$P=\sum_{i=1} P_i V_{fi}, \tag{7}$$

where P_i and V_{fi} are the material properties and volume fraction of the constituent material i, and the sum of the volume fractions of all the constituent materials makes 1.

As mentioned previously the effective properties like thermal expansion coefficient α, and thermal conductivity k are assumed to be temperature dependent and thus can be expressed as a nonlinear function of temperature [12]:

$$P_i=P_0(P_{-1}T^{-1}+1+P_1T+P_2T^2+P_3T^3), \tag{8}$$

where P_0, P_{-1}, P_1, P_2 and P_3 are the coefficients of temperature T (in K) and are unique to the constituent materials. The typical values for thermal expansion coefficient α (in 1/K), the thermal conductivity k (in W/m.K) and specific heat capacity c (in J/Kg.K) of ceramics and metals are listed in Ref. [12].

In this study, the simple rule of mixture is used to predict the material property $P(r, z, T(r, z, t))$ at any arbitrary point (r, z) for the 2D-FGM cylinder. The linear combination of

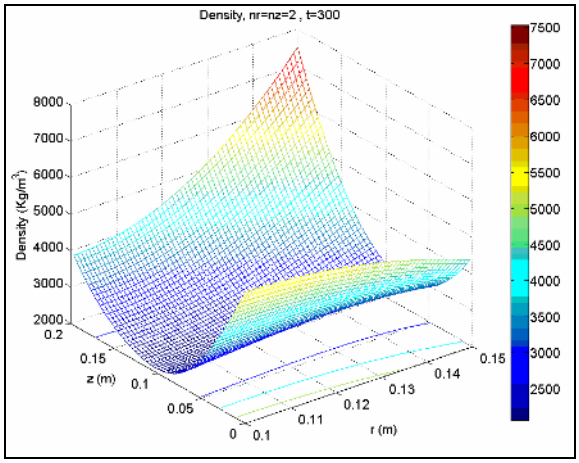

Fig. 2. The variation of density through the cylinder for the typical values of $n_r = 2$ and $n_z = 2$ after 300 second.

volume fractions and material properties of the basic materials is shown in the following equation:

$$P(r,z,T(r,z,t)) = P_{c1}(T(r,z,t))V_{c1}(r,z) + P_{c2}(T(r,z,t))V_{c2}(r,z) + P_{m1}(T(r,z,t))V_{m1}(r,z) + P_{m2}(T(r,z.t))V_{m2}(r,z). \quad (9)$$

This method is simple and convenient to apply for predicting the overall material properties and responses; however, owing to the assumed simplifications the validity is affected by the detailed graded microstructure.

The variation of a material property, such as density based on the mentioned approach through the cylinder for the typical values of $n_r = 2$ and $n_z = 2$ after 300 second is shown in Fig. 2.

2.3 Graded finite element modelling

Graded elements can be compared with conventional homogeneous elements such as those ones used in traditional layered analysis of FGMs. It would be noted that the graded element incorporates the material property gradient at the scaling size of the element, while the homogeneous element produces a stepwise constant approximation for a continuous material property field. The special effects of these discontinuities will be more considerable in the 2D-FGMs because of its 2D non-homogeneity. Besides, the graded elements are implemented by means of direct sampling properties at the Gauss points of the element [34, 37], as illustrated by Fig. 3. Based on these facts, the graded finite element is strongly preferable for modelling the present problem.

To model the heat transfer problem, an axisymmetric ring element with rectangular cross-section is used to discretize the domain. By taking into account the nine nodal values of temperature as the freedom degree, the quadratic interpolation model can be derived as [38]:

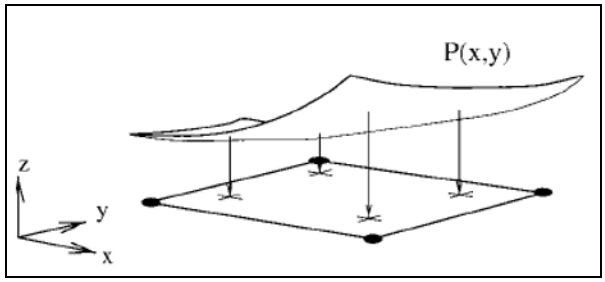

Fig. 3. Graded element with direct sampling of properties at the Gauss points [34, 37].

$$T^e(r,z,t) = [N_i(r,z)]\{q_i(t)\}^e, \quad i = 1,2,\ldots,9, \quad (10)$$

where $[N_i(r,z)]$ is the matrix of quadratic interpolation functions and $\{q(t)\}^e$ is the nodal temperature vector of the nine node element. Additional information is provided in the Appendix.

The weak form of the present problem leads to the following integral:

$$0 = \iiint_V \left[k(r,z,T(r,z))\left(\frac{\partial T}{\partial r}\right)^2 + k(r,z,T(r,z))\left(\frac{\partial T}{\partial z}\right)^2 + 2\rho cT\left(\frac{\partial T}{\partial t}\right)\right] dv + \iint_S h(T^2 - 2TT_\infty), \quad (11)$$

where v and s are the volume of the cylinder and the boundary on which the convective heat transfer is specified. This weak form in which the coefficient of thermal conductivity is dependent on r, z and T, is the sum of elemental quantities. By considering the initial and boundary conditions, the graded finite element equation for whole domain is concluded as:

$$[\mathrm{K_M}]\{\dot{\mathrm{Q}}\} + [\mathrm{K}]\{\mathrm{Q}\} = \mathrm{F_T}, \quad (12a)$$

where $\{\mathrm{Q}\}$ is the vector of cylinder nodal temperature and also:

$$[\mathrm{K_M}] = \sum_{e=1}^{m}[\mathrm{k_m}]^e, \quad (12b)$$
$$[\mathrm{K}] = \sum_{e=1}^{m}([\mathrm{k_1}]^e + [\mathrm{k_2}]^e), \quad (12c)$$
$$\mathrm{F_T} = \{\mathrm{f_T}\}^e, \quad (12d)$$

where m is the number of elements. For finding the characteristic matrices, the integral must be applied over the elemental volume by considering the distribution function of material properties through each element. According to Eq. (11), the finite element equations for each element are depicted as:

$$[\mathrm{k_m}]^e\{\dot{q}\}^e + [\mathrm{k_1}]^e\{q\}^e + [\mathrm{k_2}]^e\{q\}^e = \{\mathrm{f_T}\}^e, \quad (13a)$$

where

$$[k_m]^e = \iiint_v \rho c\{N\}^T\{N\}dv, \quad (13b)$$

$$[k_1]^e = \iiint_v [B]^T[D][B]\,dv, \quad (13c)$$

$$[k_2]^e = \iint_s \{N\}^T h\{N\}\,ds, \quad (13d)$$

$$\{f_T\}^e = \iint_s hT_\infty\{N\}^T ds, \quad (13e)$$

$$[B] = \begin{bmatrix} \frac{\partial N_1}{\partial r} & \cdots & \frac{\partial N_9}{\partial r} \\ \frac{\partial N_1}{\partial z} & \cdots & \frac{\partial N_9}{\partial z} \end{bmatrix}, \quad (13f)$$

$$[D] = \begin{bmatrix} k(r,z,T) & 0 \\ 0 & k(r,z,T) \end{bmatrix}. \quad (13g)$$

By assembling the elements of matrices, the global matrix equation for the structure can be obtained like Eq. (12a). This set of equations is time dependent and highly nonlinear, and thus the solving methodology for large set of equations like this form needs a procedure in which the time dependency is given by a finite difference approximation [38] and the nonlinear solver uses an affine invariant form of the damped Newton method as described in Ref. [39].

After mesh dependency analysis, 4000 elements illustrated very good convergence and no change in the results by increasing the number of elements. This number of elements was achieved by dividing the cylinder into 40 elements across the radial direction and 100 elements across the axial directions.

3. Implementation and validation

To verify the present study, since the similar works are done only in few cases, a similar problem in the literature was chosen. The present problem is simplified to be close to the published literature, as in this example results are derived for the very special case of the classical thermoelasticity wherein the transient temperature distribution is considered. An axisymmetric, thermoelastic boundary value problem is solved for a functionally gradient cylinder with an inner radius of 0.0127 m and an outer radius of 0.0254 m. It was assumed that the cylinder was too long and the heat conduction phenomenon occurred in one dimension. The effects of the temperature-dependency of the material properties on the results are also considered. In this regard, Si_3N_4/SUS304 cylinder with a ceramic-rich inner layer and a metal-rich outer layer was considered; the volume fraction distribution was chosen in terms of a power-law (n).The temperature-dependent material properties are given in Ref. [12].

All points of the cylinder are initially at the ambient temperature of 298.15K. The inner surface of the cylinder is suddenly subjected to a convection heat transfer with a passing medium with 2000K temperature and h = 750 W/m^{2}K. Therefore, the boundary conditions are expressed as [12]:

$$2\pi r\left[k\frac{\partial T}{\partial r} + h_c(T - T_\infty)\right] = 0 \text{ at } r=r_i, \quad (14a)$$

$$2\pi r k\frac{\partial T}{\partial r} = 0 \text{ at } r=r_o. \quad (14b)$$

The temperature distribution at the inner surface of the cylinder as a function of time for two power exponents (n = 1.0, and 25.0) is shown in Fig. 4.

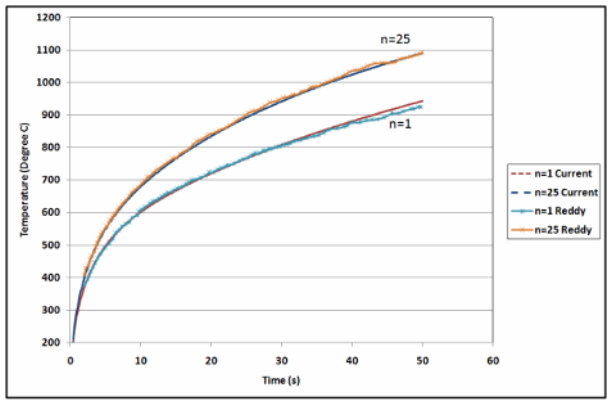

Fig. 4. The temperature distribution at the inner surface of the cylinder as a function of time for two power exponents present and Reddy study (n = 1.0, and 25.0).

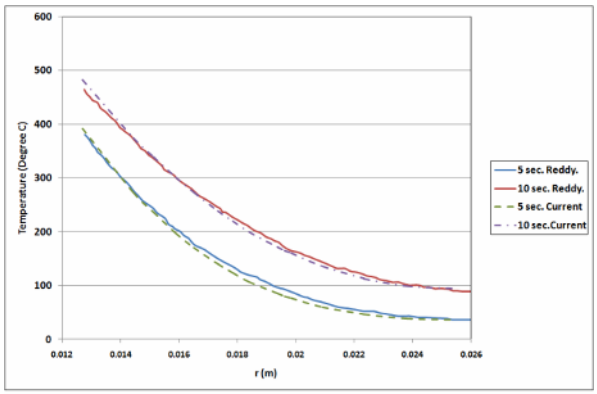

Fig. 5. The comparison of the temperature distribution plots for 5 and 10 seconds along the cylinder radius (present and Reddy study).

In this figure, the results from the present study are compared with the Reddy and Chen's work [12]. It is obvious that these curves are completely the same and they have very good agreement with each other.

In addition, the transient temperature distributions are plotted along the radius in different times for power exponents zero (n = 0), which means that the cylinder is made of homogeneous SUS304 material thoroughly. Fig. 5 shows the comparison of the temperature distribution plots for 5 and 10 seconds along the cylinder radius.

Finally, regarding the comparison of the driven results from the present study and those extracted from the Reddy and Chin study, which is shown in Figs. 4 and 5, it can be determined that the achieved results from the new investigation are verified.

4. Results and discussion

A thick hollow cylinder of inner radius a = 0.1 m, outer radius b = 0.15 m, and length of L = 0.2 m made of 2D-FGM which the gradation of the material distribution profile is in

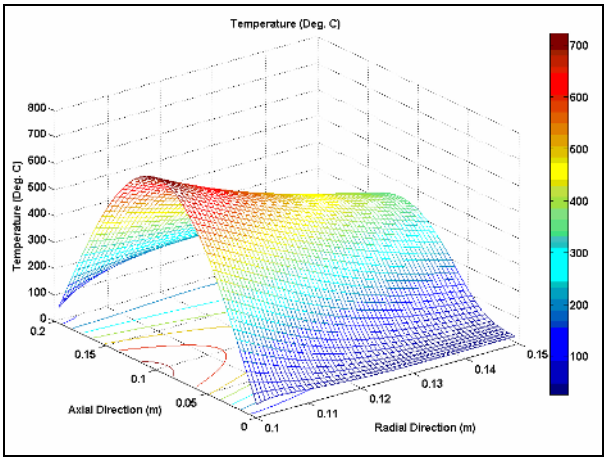

Fig. 6. The temperature distribution among the cylinder wall after 100 seconds ($n_r = n_z = 2$).

two direction was considered.

Constituent materials are two distinct ceramics and two distinct metals described as $c1 = Zirconia$, $c2 = Aluminum.Oxide$, $m1 = Ti \cdot 6Al \cdot 4V$ and $m2 = Stainless.Steel$ which is the temperature dependent material properties are explained in Ref. [12]. The volume fraction of these materials is distributed according to the Eq. (6).

The boundary conditions are expressed as:

$$T(r = 0.1, z, t) = 700(1 - e^{-2t})\sin\left(\frac{\pi z}{L}\right) \quad (15a)$$

$$k\frac{\partial T(r=0.15,z,t)}{\partial r} + h_0(T - T_\infty) = 0 \quad (15b)$$

$$-k\frac{\partial T(r,z=0,t)}{\partial z} + h_L(T - T_\infty) = 0 \quad (15c)$$

$$\frac{\partial T(r,z=0.2,t)}{\partial z} = 0 \quad (15d)$$

where Eqs. (15a)-(15d) show temperature at the inner radius and heat convection at the outer and lower surface respectively. h_0 and h_L are equal to 150W/(m^2. ˚K) in the outer side and lower surfaces, respectively, and thermal isolation at upper surface. T_∞ = 25˚C is the surrounding temperature and this cylinder exposed to the initial uniform temperature of 25˚C.

The temperature distribution among the cylinder wall after 100 second is shown in the Fig. 6. In The power law exponents of the material distribution profile in radial and axial directions are the same, $n_r = n_z = 2$.

The transient heat transfer and temperature dependency of material properties besides the volume fraction variation of those properties in two dimensions all in interconnection with each others lead to different temperature distribution in the cylinder. Among these parameters, the variation of thermal properties in two dimensions and temperature dependency of them cause considerable changes in cylinder temperature contours.

The effect of the variation of the material distribution along r-direction after 600 seconds on cylinder temperature distribution is shown in Fig. 7. It is obvious that there are no significant changes for temperature distribution across the cylinder wall due to the power exponent increasing along the r-direction.

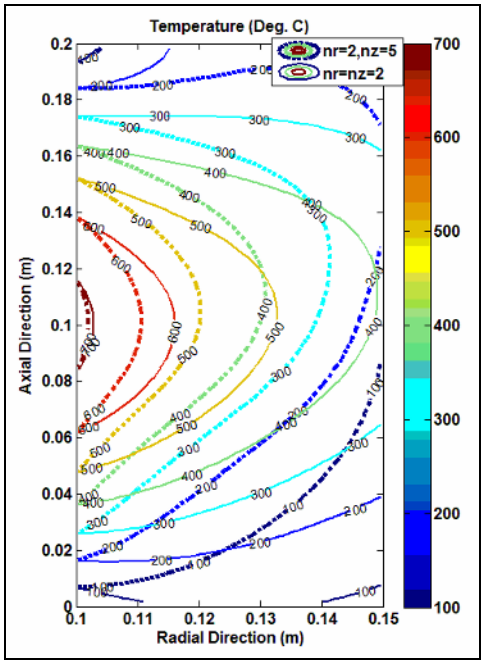

Fig. 7. The effect of the variation of the material distribution along r-direction after 100 second on cylinder temperature distribution.

In the other contour, the effect of power exponent variation in z-direction leads to significant change in the cylinder temperature distribution. The increasing of the n_z leads to lower temperature distribution through the cylinder wall after 600 second (Fig. 8).

Figs. 9 and 10 demonstrate interesting results; where after 1200 second along the horizontal center line of cylinder wall as shown in Fig. 9, the variation of material distribution in r-direction does not have any changes on temperature along this line, although just in the case when there is no change in r-direction ($n_r = 0$). In fact, for $n_r = 0$, the temperature along the horizontal centerline is lower than the other variation in values of n_r (Fig. 9).

Fig. 10 shows n_z variation along the centerhorizontal line of the cylinder wall after 1200 seconds.

By increasing the value of n_z, the temperature along the centerline is decreasing significantly, in which when there is no material variation along the r-direction. The highest temperature will be achieved along the centerline in comparison with the material variation ones. The difference is about 505 degrees of centigrade from $n_z = 0$ to $n_z = 15$.

The time response of temperature at the points 1, 2, and 3 specified in Fig. 1 is illustrated in Figs. 11 and 12. It is clear that the time response of temperature at these points is strongly affected by material composition. The time response of temperature at point 1(P_1) shows that in the same material

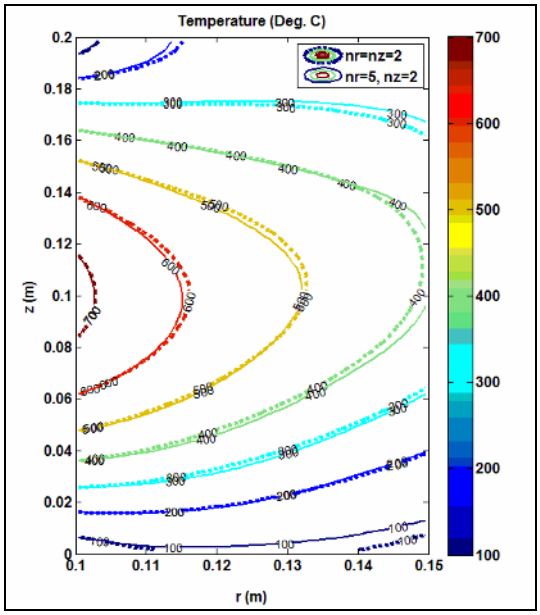

Fig. 8. The effect of the variation of the material distribution along z-direction after 600 second on cylinder temperature distribution.

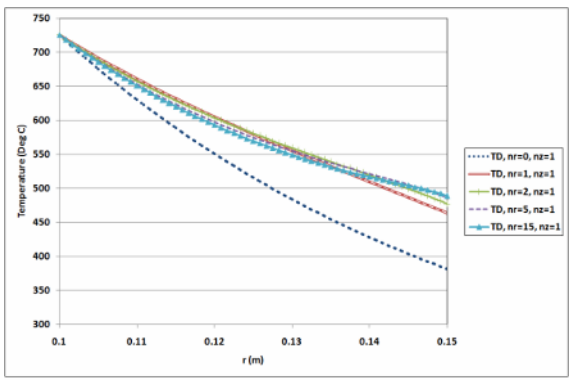

Fig. 9. Temperature along the horizontal center line of cylinder wall after 1200 seconds.

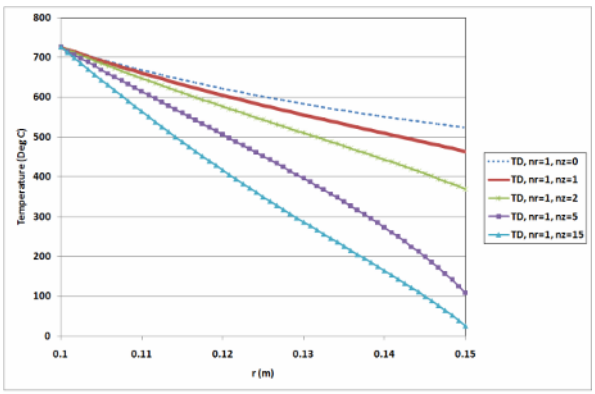

Fig. 10. Temperature along the centerhorizontal line of the cylinder wall after 1200 seconds.

distribution in z-direction by increasing the n_r, the temperature

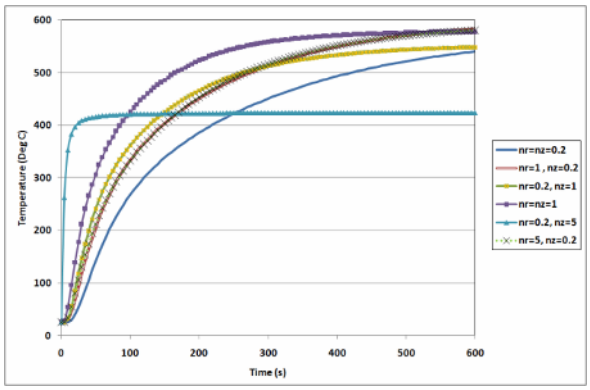

Fig. 11. The time response of temperature at point 1(p1).

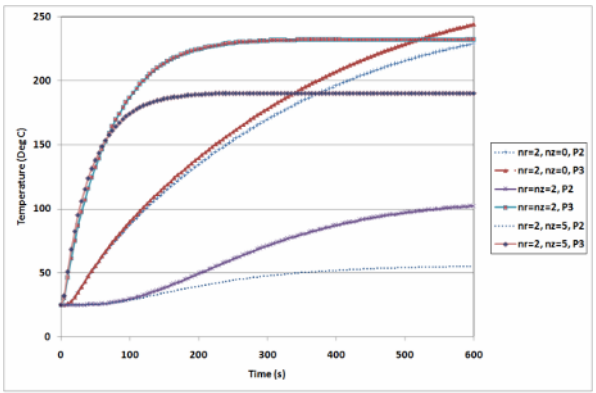

Fig. 12. The time response of temperature for two points (p2 and p3) with different power exponent n_z.

values are enhanced (Fig. 11). By increasing the value of n_z from 0.2 to 5, the temperature becomes steady earlier and thus the steady temperature becomes lower.

Furthermore, it is interesting that the results with $n_r = 5$ and nr = 0.2 coincided with the results of $n_r = 1$ and $n_z = 0.2$, which demonstrates when $n_z = 0.2$ the variation of material along radial direction leads to no change in temperature on the "point 1."

The time response of temperature for two points (p_2 and p_3) with different power exponent n_z with $n_r = 2$ is illustrated in Fig. 12. For point (p_2) the temperature vs. time is decreasing by increasing of n_z which is not seen for P_3. For both points (p_2 and p_3) increasing of n_z leads to take place earlier with lower steady temperature.

Because of using FGMs in the components which encounter high level of temperature load, neglecting of the temperature dependency for material properties leads to inaccurate results. In Figs. 13 and 14 the temperature contours of TD and TID of the material properties for two different time frames (100 and 300 seconds) and the same material distribution are depicted. The difference between TD and TID contours is increasing by passing time. It is interesting that the TD contours estimate more temperature value than TID one, which will be

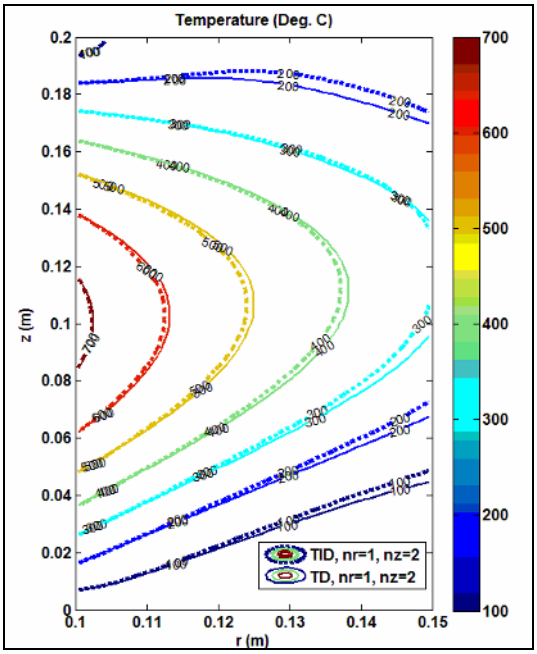

Fig. 13. Temperature contours of TD and TID of the material properties after 100 seconds.

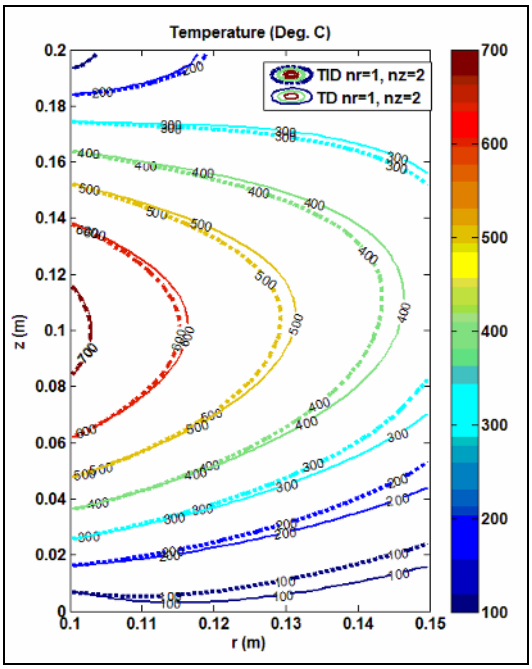

Fig. 14. Temperature contours of TD and TID of the material properties after 300 seconds.

important for designers to evaluate the ability of components to withstand severe thermal shocks. For the same material distribution (n_r = 1 and n_z = 2), after 100 seconds using TID material properties leads to 11% error in the temperature distribution across the cylinder wall, and after 300 seconds it will increase to the value of 20% . These error values show the importance of utilizing the temperature dependency of the

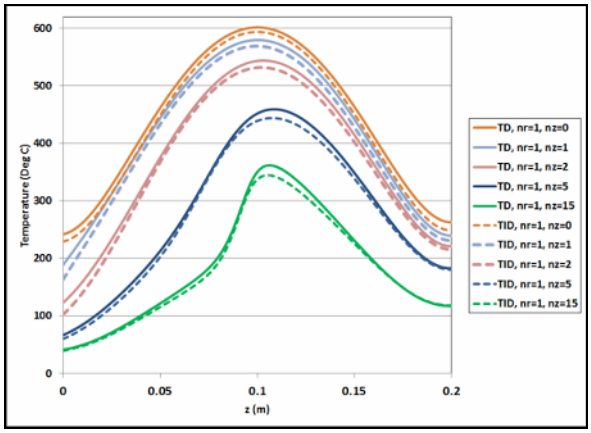

Fig. 15. Temperature distribution along the vertical center line of cylinder (TD and TID).

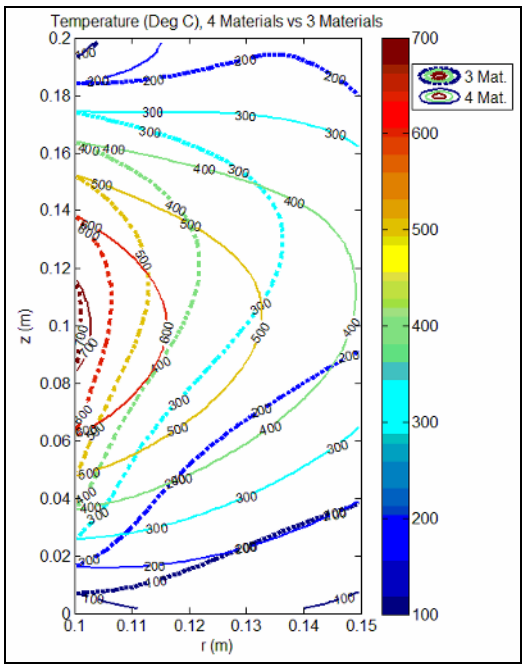

Fig. 16. Comparison of the temperature distribution contour for 3 and 4 materials FGM with the same material distributions.

materials.

For evaluating the effect of material distribution along z-direction and temperature dependency of material properties, temperature distributions along the vertical centerline of the cylinder are demonstrated in Fig. 15. The TD curves show high temperature values in all material distribution, and by increasing the power exponent (n_z) the temperature values along this line are decreasing extensively. When there is no material distribution variability in z-direction (n_z = 0), with the highest material change in z-direction (n_z = 15), the difference is 240 degrees centigrade on the TD curves.

2D-FGMs usually consist of three or four materials. Fig. 16 compares the temperature distribution contour for three mate-

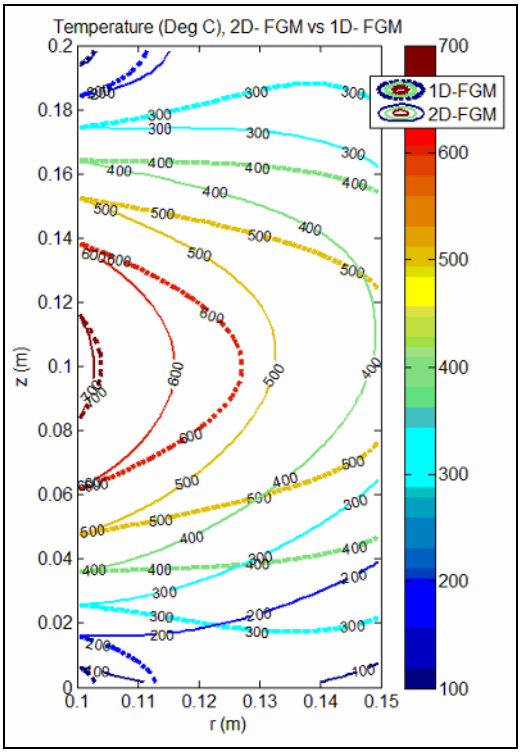

Fig. 17. Comparison of the temperature distribution contour for 1D and 2D- FGM with the same material distributions.

rials (ZrO_2, Al2O3 / SUS304) and four materials FGM with the same material distribution. The temperature contours are different with each other's and in this case four material FGMs show higher temperature in comparison with three material one.

As mentioned before, the material distribution along the other direction (z) gives more functionality to control the temperature distributions in a region. Fig. 17 compares the 1D-FGM (Al_2O_3 / SUS304) with 2D-FGM temperature distribution with the same material distribution in r-direction. Higher temperature values in the center of the cylinder and lower temperature values along the upper and lower boundaries of cylinder wall than 1D-FGM ones are the characteristics of 2D-FGM used in this case.

5. Conclusion

A graded finite element transient heat conduction analysis for a thick hollow 2D-functionally graded cylinder with finite length and temperature-dependent material properties was performed and the results were verified with a similar example in the relevant literature.

The variation of material properties in two dimensions, the graded finite element with second-order Lagrange shape functions and the nonlinear temperature dependency of the material properties are the novelty of this study. Moreover, the results based on the material distribution graph and time variation of the temperature in different power law coefficients and assumptions of temperature-dependency (TD) and temperature-independency (TID) of the material properties were compared with each other and the effects of various parameters on the transient responses were demonstrated.

For the same material distribution (n_r = 1 and n_z = 2) after 100 seconds using TID material properties leads to 11% error in the temperature distribution across the cylinder wall, and also after 300 seconds it increases to the value of 20% . These error values show the importance of utilizing the temperature dependency of the materials in the transient heat conduction analysis.

Increasing of $n_z$in all cases leads to achieve early steady and lower temperature distributions, but by increasing the n_r brings about no significant changes in temperature distribution.

Finally, the 2D-FGMs prove their high capabilities in reducing the temperature more so than conventional FGM if suitable distributions of the material properties are employed.

Nomenclature

a, b	: Inner and outer radii
2c, 2d	: Element length in r and z- direction
c(r, z, T)	: Heat capacity of functionally graded material
c_0	: Constant value
c1, c2	: First ceramic and second ceramic
h_L, h_o, h_U	: Convection coefficients at lower, outer and upper surfaces
$k_r(r, z)$, $k_z(r, z)$	: Thermal conductivity in the radial and axial directions
$[k_1]^e$, $[k_2]^e$, $[k_m]^e$	: Characteristic matrices of elements
$[K_M]$, *[K]*	: Global characteristic matrices
[N(r, z)]	: Matrix of linear interpolation functions
n_r, n_z	: Radial and axial power law exponents
m1, m2	: First metal and second metal
P(x,y)	: General material properties
$\{q\}^e$	: Nodal temperature vector of element
{Q}	: Global nodal temperature
r_c *and* z_c	: Coordinates of the element centroid
T_o	: Constant value
T_∞	: Surrounding temperature
$V_{c1}, V_{c2}, V_{m1}, V_{m2}$	: Volume fractions of basic materials
$\rho(r, z, T)$	: Mass density of functionally graded material
ξ and η	: Non-dimensional element local coordinate

References

[1] N. Noda, Thermal stresses in functionally graded materials, *J. Therm. Stresses*, 22 (1999) 477-512.

[2] B. D. Choules and K. Kokini, Architecture of functionally graded ceramic coating against surface thermal fracture, *ASME J. Eng. Mater. Technol*., 118 (1996) 522-528.

[3] N. Noda, Thermal stresses in materials with temperature-dependent properties, *Appl. Mech. Rev*., 44 (1991) 83-97.

[4] Y. Tanigawa, Some basic thermoelastic problems for non-

homogeneous structural materials, *Appl. Mech. Rev*., 48 (1995) 287-300.

[5] R. W. Zimmerman and M. P. Lutz, Thermal stress and thermal expansion in a uniformly heated functionally graded cylinder, *J. Therm. Stresses*, 22 (1999) 88-177.

[6] Y. Obata and N. Noda, Steady thermal stresses in a hollow circular cylinder and a hollow sphere of a functionally gradient material, *J. Therm. Stresses*, 17 (1994) 471-487.

[7] N. El-abbasi and S. A. Meguid, Finite element modeling of the thermo elastic behaviour of functionally graded plates and shells, *Int. J. Comput. Eng. Sci*., 1 (2000) 51-165.

[8] M. Jabbari, S. Sohrabpour and M. R. Eslami, Mechanical and thermal stresses in a functionally graded hollow cylinder due to radially symmetric loads, *Int. J.Press. Vess. Pip*., 79 (2002) 493-497.

[9] M. Jabbari, S. Sohrabpour and M. R. Eslami, General solution for mechanical and thermal stresses in a functionally graded hollow cylinder due to non-axisymmetric steady-state loads, *ASME J. Appl. Mech*.,70 (2003) 111-118.

[10] K. M. Liew, S. Kitipornchai, X. Z. Zhang and C. W. Lim, Analysis of the thermal stress behaviour of functionally graded hollow circular cylinders, *Int. J. Solids Struct*., 40 (2003) 2355-2380.

[11] H. S. Shen, Thermal post buckling behaviour of functionally graded cylindrical shells with temperature-dependent properties, *Int. J. Solids Struct*, 41 (2004) 1961-1974.

[12] J. N. Reddy and C. D. Chin, Thermomechanical analysis of functionally graded cylinders and plates, *J. Therm. Stresses*, 21 (1998) 593-626.

[13] Y. Ootao and M. Ishiharaa, Transient thermal stress problem of a functionally graded magneto-electro-thermoelastic hollow cylinder due to a uniform surface heating, *Journal of Thermal Stresses*, 35 (6) (2012) 517-533.

[14] H. L. Lee, W. J. Chang, S. H. Sun and Y. Ch. Yang, Estimation of temperature distributions and thermal stresses in a functionally graded hollow cylinder simultaneously subjected to inner-and-outer boundary heat fluxes, *Composites Part B: Engineering*, 43 (2) (2012) 786-792.

[15] S. M. Hosseini and M. H. Abolbashari, Analytical solution for thermoelastic waves propagation analysis in thick hollow cylinder based on green-naghdi model of coupled thermoelasticity, *Journal of Thermal Stresses*, 35 (4) (2012) 63-37.

[16] T. Darabseh, N. Yilmaz and M. Bataineh, Transient thermoelasticity analysis of functionally graded thick hollow cylinder based on Green-Lindsay model, *Int. J. Mech. Mater*., 8 (2012) 247-255.

[17] X. D. Zhang, Y. L Hong and A. H Li, Optimization of axial symmetrical FGM under the transient-state temperate field, *International Journal of Minerals, Metallurgy and Materials*, 19 (1) (2012) 59.

[18] H. Awaji and R. Sivakumar, Temperature and stress distribution in a hollow cylinder of functionally graded material: The case of temperature-independent material properties, *J. Am. Ceram. Soc*., 84 (2001) 1059-1065.

[19] K. S. Kim and N. Noda, Green's function approach to unsteady thermal stresses in an infinite hollow cylinder of functionally graded material, *Acta Mech*., 156 (2002) 145-161.

[20] J. Sladek, V. Sladek and C. Zhang, Transient heat conduction analysis in functionally graded materials by the meshless local boundary integral equation method, *Comput.Mater. Sci*., 28 (2003) 494-504.

[21] B. L. Wang, Y. W. Mai and X. H. Zhang, Thermal shock resistance of functionally graded materials, *ActaMater*., 52 (2004) 4961-4972.

[22] B. L. Wang and Y. W. Mai, Transient one-dimensional heat conduction problems solved by finite element, *Int. J. Mech. Sci.*, 47 (2005) 303-317.

[23] S. M. Hosseini, M. Akhlaghi and M. Shakeri, Transient heat conduction in functionally graded thick hollow cylinders by analytical method, *Heat Mass Trans.*, 43 (2007) 669-675.

[24] Z. S. Shao, T. J. Wang and K. K. Ang, Transient thermomechanical analysis of functionally graded hollow circular cylinders, *J. Therm. Stresses*, 30 (1) (2007) 81-104.

[25] Z. S. Shao and G. W. Ma, Thermo-mechanical stresses in functionally graded circular hollow cylinder with linearly increasing boundary temperature, *Compos. Struct*., 83 (2008) 259-265.

[26] Y. S. Touloukian, *Thermophysical properties of high temperature solid materials*, McMillan, New York (1967).

[27] M. Shariyat, S. M. H. Lavasani and M. Khaghani, Nonlinear transient thermal stress and elastic wave propagation analyses of thick temperature-dependent FGM cylinders, Using A Second-Order Point-Collocation Method, *Appl. Math. Model*, 34 (2010) 898-918.

[28] M. Shariyat, M. Khaghani and S. M. H. Lavasani, Nonlinear thermoelasticity, vibration, and stress wave propagation analyses of thick FGM cylinders with temperature-dependent material properties, *Eur. J. Mech. A. Solids*., 29 (2010) 378-391.

[29] M. Shariyat, Nonlinear transient stress and wave propagation analyses of the FGM thick cylinders, Employing a Unified Generalized Thermoelasticity Theory, *Int. J. Mech. Sci*., 65 (1) (2012) 24-37.

[30] J. R. Cho and D. Y. Ha, Optimal tailoring of 2D volume-fraction distributions for heat-resisting functionally graded materials using FDM, *Comput. Method Appl. Mech. Eng.*, 191 (2002) 3195-3211.

[31] J. Abudi and M. J. Pindera, Thermoelastic theory for the response of materials functionally graded in two directions, *Int. J. Solid Struct*., 33 (1996) 931-966.

[32] M. Nemat-Alla, Reduction of thermal stresses by developing two dimensional functionally graded materials, *Int. J. Solids Struct*., 40 (2003) 7339-7356.

[33] M. Nemat-Alla, Kh.I.E. Ahmed, I. Hassab-Allah, Elastic-plastic analysis of two-dimensional functionally graded materials under thermal loading, *Int. J. Solids Struct*., 46 (2009) 2774-2786.

[34] M. H. Santare and J. Lambros, Use of a graded finite element to model the behaviour of non-homogeneous materials, *J. Appl. Mech*., 67 (2000) 819-822.

[35] M. Asgari and M. Akhlaghi, Transient heat conduction in two-dimensional functionally graded hollow cylinder with finite length, *Heat Mass Transfer*, 45 (2009) 1383-1392.
[36] H. S. Shen, *Functionally graded materials: Nonlinear analysis of plates and shells*, CRC Press, Taylor & Francis Group (2009).
[37] J. H. Kim and G. H. Paulino, Isoparametric graded finite elements for non-homogeneous isotropic and orthotropic materials, *ASME J. Appl. Mech*., 69 (4) (2002) 502-514.
[38] O. C. Zienkiewicz and R. L. Taylor, The finite element method, 5th edn. VII: Solid mechanics, Elsevier Ltd. (2000).
[39] P. Deuflhard, A modified newton method for the solution of ill-conditioned systems of nonlinear equations with application to multiple shooting, *Numer. Math.*, 22 (1974) 289-315.

Appendix A

The matrix of Lagrange interpolation functions is [38]:

$$N_i(r,z) = \{N_1(r,z), N_2(r,z), \dots, N_9(r,z)\}. \quad \text{(A.1)}$$

A local coordinate system is defined for each Lagrange rectangle element to facilitate the derivation of the shape functions. The r_c and z_c are the coordinates of the element centroid and the length of element in r- direction is $2c$ and in z- direction is $2d$. Note that in the local coordinate system the rectangular element becomes a square of side equal to two [38].

$$N_i = \frac{1}{4}(\xi^2 + \xi\xi_i)(\eta^2 + \eta\eta_i) i = 1,3,5,7, \quad \text{(A.2a)}$$

$$N_i = \frac{1}{2}\eta_i{}^2(\eta^2 + \eta\eta_i)(1-\xi^2) + \frac{1}{2}\xi_i{}^2(\xi^2 + \xi\xi_i)(1-\eta^2) \quad i = 2,4,6,8, \quad \text{(A.2b)}$$

$$N_9(\xi,\eta) = (1-\xi^2)(1-\eta^2), \quad \text{(A.2c)}$$

$$\xi = \frac{r-r_c}{c} \quad ; \quad \eta = \frac{z-z_c}{d}. \quad \text{(A.2d)}$$

Vector of nodal temperature (degrees of freedom) is [38]:

$$\{q_i\}^e = \begin{Bmatrix} T_1 \\ T_2 \\ \cdot \\ \cdot \\ T_9 \end{Bmatrix}. \quad \text{(A.3)}$$

Mohammad Hasan Shojaeefard is a Professor and Head of Automotive Eng. Research Center (AERC) & Automotive Eng. Dept (AED) in the Iran University of Science and Technology. His work is relating to automotive engineering (vehicle engine and body design). His work also is dedicated to research in the field of Mechanical and Automotive Engineering and training of the students.

Amir Najibi is a Ph.D. Student of Automotive Engineering in the Iran university of Science and Technology. His work is related to vehicle body design and crashworthiness capability of structures and pedestrian safety. He is also working on the application of FGM's in the vehicle engine.